Modelled and observed sea surface fCO2 in the southern ocean

Louanchi, Ferial; Hoppema, Mario; Bakker, Dorothée C.E.; Poisson, Alain; Stoll, Michel H.C.; Baar, Hein J.W. de; Schauer, Bernard; Ruiz-Pino, Diana P.; Wolf-Gladrow, Dieter

Published in:
Tellus B

DOI:
10.1034/j.1600-0889.1999.00029.x

Publication date:
1999

Tellus (1999), 51B, 541–559
Printed in UK – all rights reserved

TELLUS
ISSN 0280–6495

Modelled and observed sea surface fCO_2 in the southern ocean: a comparative study

By FERIAL LOUANCHI[1,6]*, MARIO HOPPEMA[2], DOROTHÉE C. E. BAKKER[3], ALAIN POISSON[1], MICHEL H. C. STOLL[4], HEIN J. W. DE BAAR[4], BERNARD SCHAUER[1], DIANA P. RUIZ-PINO[1] and DIETER WOLF-GLADROW[5], [1]*Laboratoire de Physique et Chimie Marines, UPMC-CNRS URA 2076, case 134, 4 place Jussieu, 75252 Paris cedex 05, France;* [2]*University of Bremen, FB1, IUP, Dept. Tracer Oceanography, PO Box 330 440, D–28334 Bremen, Germany;* [3]*Laboratoire d'Océanographie DYnamique et de Climatologie, CNRS/ORSTOM/UPMC, case 100, 4 place Jussieu, 75252 Paris cedex 05, France;* [4]*Netherlands Institute for Sea Research, PO Box 59, 1790 AB Den Burg, Texel, The Netherlands;* [5]*Alfred Wegener Institute for Polar and Marine Research, Am Handelshafen 12, D–27570 Bremerhaven, Germany*

(Manuscript received 9 December 1997; in final form 25 September 1998)

ABSTRACT

The results of an existing one-dimensional diagnostic model that calculates the fugacity of CO_2 (fCO_2) in the surface layer of the southern ocean were compared with in situ observations from different ocean sectors and seasons. Our model is based on the translation of monthly variations of constraints fields into surface water fCO_2 variations, and was used to assess the CO_2 uptake of the southern ocean. In situ observations are useful to verify the model results and were here applied to improve the estimation of the CO_2 uptake of the southern ocean south of 50°S. The model reproduces the fCO_2 distribution in both Pacific and Indian sectors of the southern ocean satisfactorily, the mean deviation being only 5 μatm. This discrepancy requires only a minor modification of the CO_2 uptake calculated by the model for that area. By contrast, the model strongly underestimates the fCO_2 levels in early spring and early winter in the Weddell gyre. This indicates that the CO_2 uptake by the Atlantic sector of the southern ocean as calculated by the model, amounting to 0.47 GtC yr^{-1}, should be reduced, possibly by about half of this value. The reason for this mismatch lies in the use of climatological physical constraints by the model, that do not sufficiently well describe reality. Partly, the mismatch is also caused by a difference of seasonal stage between the model which reflects climatological conditions and the real ocean which is affected by interannual variability. Based on this study it is concluded that the CO_2 uptake of the southern ocean south of 50°S is likely to lie somewhere between 0.6 and 0.7 GtC yr^{-1} for the 1990s, which is a high value compared to estimates from other investigations.

1. Introduction

Since the beginning of the industrial era, the CO_2 content of the atmosphere has grown due to the combustion of fossil fuel (Keeling et al., 1989). Because CO_2 is a greenhouse gas, this increase has likely had an impact on climate. Since 1958 atmospheric CO_2 has been monitored at several stations throughout the world in such a way that the variability is known with a reasonable space/time coverage (Keeling et al., 1995; Masarie and Tans, 1995). At the beginning of the 1990s, the release of fossil fuel CO_2 to the atmosphere was about 6 GtC yr^{-1} (1 GtC = 1 Gton C =

* Corresponding author.
E-mail: louanchi@ccr.jussieu.fr, ferial@essc.psu.edu. new at: 6 The Pennsylvania State University, Department of Meteorology, 419 Walker Building, University Park, PA 16802, USA.

10^{15} g C), whereas the atmospheric CO_2 concentration was growing by only 3.4 GtC yr^{-1} (Conway et al., 1994). About half of the fossil fuel input disappears every year, being absorbed by the oceans and the terrestrial biosphere. One of the challenges for the scientific community is to identify and quantify the oceanic and terrestrial CO_2 sinks along with the processes responsible for this. The quantification of the part absorbed by these reservoirs is difficult since carbon is the basis of all terrestrial and oceanic biogeochemical cycles, giving rise to a large natural variation of CO_2 in these reservoirs.

The global carbon budget is not well-balanced; actually, the magnitude of the known sources is larger than that of the known sinks of CO_2 which is commonly referred to as the problem of the "missing sink" (Sarmiento and Sundquist, 1992). Recently, investigators questioned the current global carbon budget using atmospheric models as a basis to deduce oceanic and terrestrial source and sink distributions (Tans et al., 1990; Ciais et al., 1995; Denning et al., 1995). They contend that the oceanic CO_2 sink is more than a factor two smaller than previously assumed and invoked a large CO_2 sink in the terrestrial biosphere of the northern hemisphere. Unfortunately, large uncertainties remain in direct quantification of the terrestrial sink (Houghton et al., 1996). Although an increasing amount of in situ observations, satellite data and models are becoming available, and new methods to add constraints to the carbon budget have been developed (Keeling et al., 1993; Tans et al., 1993), the missing sink remains a matter of debate.

Oceanic fCO_2 data are available only for restricted periods and areas (fCO_2 is the fugacity of CO_2, which by value is nearly equal to its partial pressure). The observed spatio-temporal variations of the sea surface fCO_2 are so large that integrating the derived air–sea CO_2 fluxes over larger areas and long periods becomes highly uncertain. The Oceanic general circulation models (OGCM) of carbon are thus useful to obtain a reliable value for the oceanic uptake of CO_2 on large time and space scales. The results of these models converge to about 2 ($\pm$0.8) GtC yr^{-1} (Sarmiento et al., 1992; Houghton et al., 1996). However, there are still uncertainties in the ocean circulation resulting in uncertainties in the oceanic carbon uptake particularly for the southern ocean (Orr, 1996; Sarmiento and Le Quéré, 1996). The southern ocean is the least documented ocean. It appears to be an important area for absorbing anthropogenic CO_2 and it could play a key role in the future evolution of climate (Sarmiento and Le Quéré, 1996).

In the southern ocean the observations of surface water fCO_2 show a high spatio-temporal variability (Takahashi et al., 1993; Poisson et al., 1993; Robertson and Watson, 1995; Bakker et al., 1997) and only a few data are available for the winter period (Stoll et al., 1998). To determine whether this ocean is a source or a sink for atmospheric CO_2 requires the extrapolation of the sparse available observations over a wide area and for the whole year. In this work we perform an extrapolation of fCO_2 fields derived from external forcings to obtain the air–sea CO_2 fluxes over one year south of 50°S. To improve the reliability of this estimate, the modelled fCO_2 fields are compared with observations. We use several cruises conducted in the Atlantic, Pacific and Indian sectors of the southern ocean. We will briefly describe the model used to extrapolate fCO_2 fields in the southern ocean and the main results of this modelling study. The impact of the uncertainties of the modelled fCO_2 fields on the estimate of the CO_2 uptake in the southern ocean will be discussed.

2. Model results

2.1. Model description

Louanchi et al. (1996) have developed a simple model able to diagnose sea surface fCO_2 fields on a monthly scale. The model was first validated in the Indian Ocean north of 50°S and reproduced quite well the observed seasonal and spatial variability of the surface water fCO_2. A striking feature of the model is the use of variations of the mixed-layer depth and of chlorophyll as constraints, avoiding the uncertainties linked to ocean circulation and to biological prognostic (sub)models (Sarmiento and Le Quéré, 1996). The model translates the monthly variations of constraints into monthly fCO_2 variations in a surface ocean box. The constraints are the satellite wind speed (Boutin and Etcheto, 1997), the mixed-layer depth as derived from the temperature and salinity profiles from Levitus and Boyer (1994) and Levitus

et al. (1994), the sea surface temperature (Reynolds and Marsico, 1993), the chlorophyll concentration (Chl-CZCS) (Coastal Zone Color Scanner satellite observations of sea color) and the sea-ice coverage (Gloersen et al., 1992). The model was applied on grids of 2° latitude by 2° longitude to simulate the monthly fCO_2 fields in the southern ocean south of 50°S.

The fCO_2 variations are expressed by:

$$\delta f/\delta t = (\delta f/\delta t)_B + (\delta f/\delta t)_M + (\delta f/\delta t)_F + (\delta f/\delta t)_T,$$

where $\delta f/\delta t$ is the total fCO_2 variation for a time step δt. The subscripts B, M, F and T refer to biological activity, mixing, air–sea flux and thermodynamical changes, respectively. Except for the thermodynamical effect which is calculated directly with the Goyet et al. (1993) polynomials, the variation of fCO_2 is calculated from temperature, salinity, dissolved inorganic carbon (DIC) and total alkalinity (TA) using the constants of Goyet and Poisson (1989). Each term of the above equation corresponds to a specific process and is parametrized as a function of the constraints fields monthly variations which induce monthly changes in DIC and TA state variables. A description of the model equations in terms of DIC and TA can be found in Section 7 (Louanchi et al., 1996; Metzl et al., 1998).

Running the model for the whole southern ocean requires an adequate circumpolar characterization of the subsurface layers which act as boundary conditions in this model. The depth of the pycnocline was determined from the observed profiles of the density and represents the top of the subsurface box.

As a first step, we keep the subsurface invariant all year round. This assumption is supported by the fact that at steady state, it is believed that the organic carbon exported from the surface is balanced by the losses of carbon by mixing in the intermediate waters of the ocean. Moreover, subsurface data of DIC, TA and nitrate (TIN) in the southern ocean are rather sparse. For extending the subsurface data to the whole southern ocean, the approach has been to calculate subsurface values through linear interpolation and extrapolation of property–temperature relationships. This procedure was performed with data from the GEOSECS (Bainbridge, 1981; Broecker et al., 1982; Weiss et al., 1983), INDIGO 3 (Poisson et al., 1990), CIVA1/WOCE and Polarstern ANT X/4, X/7, XIII/4 expeditions. Subsurface concentrations of DIC and TA as obtained by this procedure have standard deviations of 10 and 6.5 μmol/kg, respectively. For the whole circumpolar ocean the subsurface TIN was taken as 30.5 μmol/kg according to the observations. The thus preconditioned model is supposed to simulate conditions for the period after 1990. The molar fraction of CO_2 in the atmosphere, being $xCO_2 =$ 351.9 ppm (value corresponding to 1990 at Palmer Station), is kept constant (Conway et al., 1994). Because stability of the model is reached after three years, it is not necessary to define surface DIC, TA and TIN. The subsurface values of the properties are taken to initialize the system.

2.2. *Model ΔfCO_2 in the southern ocean*

Fig. 1 shows the ΔfCO_2 fields in the southern ocean calculated by the model for February (Fig. 1a) and August (Fig. 1b) and the seasonal variation of fCO_2 (Fig. 1c).

According to these model results the surface layer is on average undersaturated in CO_2 during the austral summer period (Fig. 1a). The strongest sinks are found in the Ross Sea with undersaturations of more than 75 μatm. Such low CO_2 values of about 200 μatm were actually also observed there during austral summer (Dunbar, personal commmunication) and are related to intense phytoplankton blooms occurring in this period. The Weddell Sea presents both super and undersaturations and this spatial variability reflects the competition between biological CO_2 uptake and dynamical CO_2 enhancement of the surface layer by mixing processes. This high spatial variability was previously observed in that area (Takahashi et al., 1993). By August, the southern ocean appears to be a sink everywhere except in some locations of the Weddel Sea and along the eastern Antarctic coast in the Pacific sector (Fig. 1b). In their recent climatology, Takahashi et al. (1997) showed that this area is a sink of CO_2 for the atmosphere all year round on average, some sources being mainly located in the seasonal ice zone (extending to about 55°S in the Atlantic sector and 58–60°S in the Pacific and Indian sectors).

The fCO_2 in the Weddell gyre increases by about 25–30 μatm from February to August (Fig. 1c), whereas in most of the Pacific and Indian

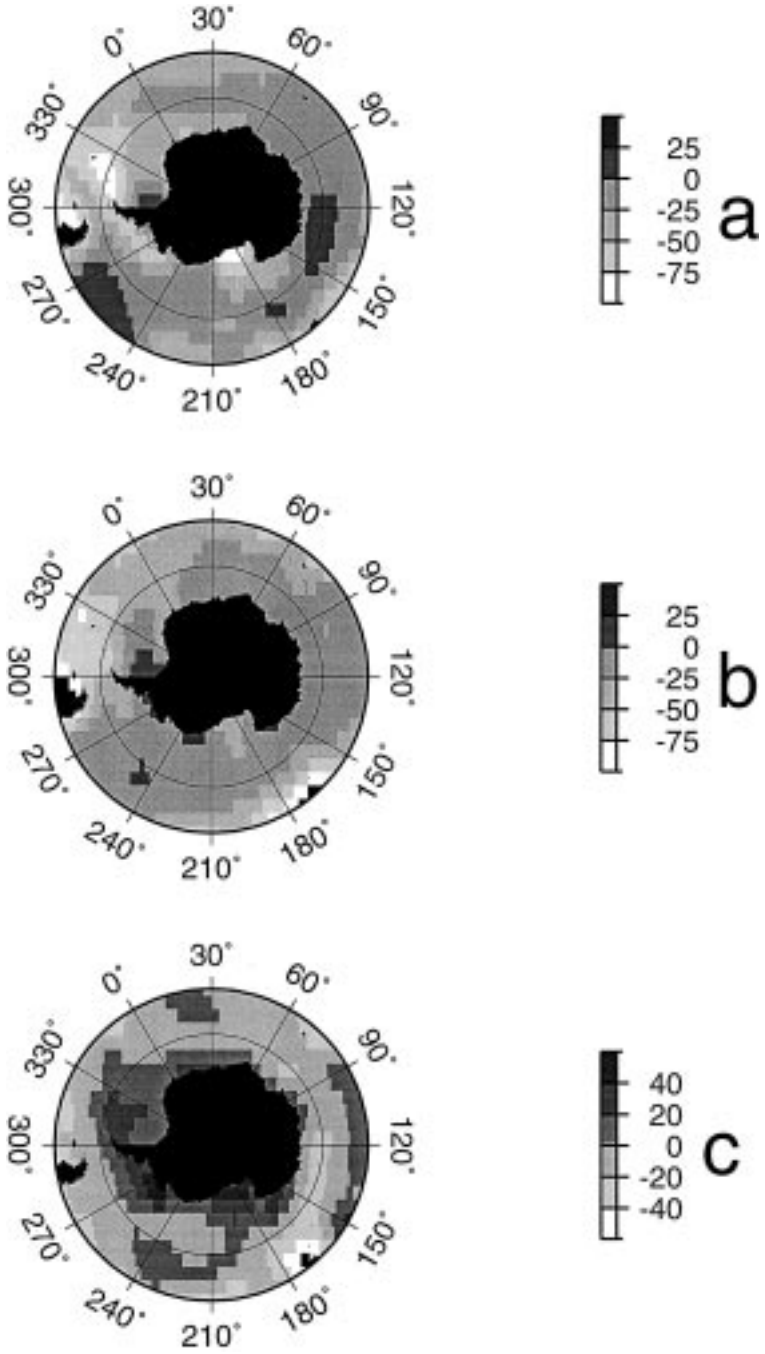

Fig. 1. Modelled values, represented as ranges for the fCO_2 difference between the surface water and the atmosphere (ΔfCO_2 in μatm) in areas of 2° latitude by 2° longitude for (a) February, (b) August and (c) seasonal variations (August minus February) in the southern ocean south of 45°S. The permanently open ocean zone is located between 50° and 58°S except in the Atlantic sector where ice may extend to 54°S. Note that the grey scale for (a) and (b) is different from that of (c).

sectors a seasonal fCO_2 decrease of about 10–15 μatm is found. More generally the observation can be made that fCO_2 increases from summer to winter in the seasonal ice zone and the polar front zone (50–52°S), whereas it decreases in the Antarctic open zone (largely covered by the Pacific and Indian sectors). The circumpolar sector has been converted into a stronger sink in winter for atmospheric CO_2 following a decrease in surface layer temperature (i.e. thermodynamical conditions). In the Indian sector the biological uptake and the mixing effect on the fCO_2 nearly cancel out on a seasonal scale, inducing "thermodynamically" mediated variations of fCO_2 (Louanchi et al., 1998). On the other hand, in the Weddell gyre low levels of CO_2 in the summer period are due to the biological uptake and the increase through the winter is due to the effect of increased mixing of subsurface water (Hoppema et al., 1995). In the Pacific sector, both situations are present. The model gives an increase of CO_2 in the Ross Sea and associated gyres, whereas the circumpolar current area presents the features described for the Indian sector. The model simulates the seasonal cycles of upper layer CO_2 according to the changes in the constraints. Results indicate that in the circumpolar current water, the biological CO_2 uptake is weak because Chl-CZCS is low in this area. The gradient between surface and subsurface waters in CO_2 is not strong enough in that case to induce significant increase of DIC during the period of mixed-layer deepening. In that situation, the solubility pump acts as the main agent of the fCO_2 seasonal change. On the other hand, in the seasonal ice zone, high Chl concentrations (greater than 1.5 mg m^{-3}) induce a strong biological pump of CO_2 during summer. From summer to winter the increase of the mixed-layer depth increases the amount of CO_2 in the surface layer. Seasonal changes in temperature are too weak in that area to compensate for the mixing effect on CO_2.

2.3. *Model air–sea CO_2 fluxes*

According to the model, the southern ocean is a substantial sink for atmospheric CO_2 of 0.9 ($\pm$0.3) GtC yr^{-1}. All sectors are CO_2 sinks on an annual basis, although certain regions within a sector may be sources for some time of the year. The Atlantic sector is the most important sink with a net uptake of 0.47 ($\pm$0.20) Gton C/yr. The Indian sector is a sink for 0.23 ($\pm$0.17) Gton C/yr while the geographically largest Pacific sector is the smallest sink with only 0.17 ($\pm$0.22) Gton C/yr. The standard deviations for these flux estimates are linked to the uncertainties in interpolation/extrapolation of the subsurface properties (see Subsection 2.1). The discrepancy between this flux estimate and previous ones which are much lower (see for example Tans et al., 1990 or Sarmiento et al., 1992 or Takahashi et al., 1997) is mainly caused by the use of satellite-derived wind speeds instead of climatological wind speeds. With a simple calculation the effect on the CO_2 uptake is illustrated of using climatological wind speed data as compared to satellite-derived data. Applying ΔpCO_2 values compiled by Tans et al. (1990) and calculating the air–sea CO_2 fluxes using satellite derived wind speeds we arrive at -0.97 and -0.32 Gton C/yr for the summer and winter periods, respectively. The fluxes were calculated using the ice-free area for both periods. The mean CO_2 uptake for the ice-free area of the southern ocean is thus 0.65 Gton C/yr, i.e. three times the estimate of Tans et al. (1990) using climatological wind speeds.

Some earlier studies integrate air–sea CO_2 fluxes from oceanic fCO_2 measurements and observed wind speeds in selected areas and periods. Murphy et al. (1991) report that the region between 50° and 60°S in the Pacific sector is a CO_2 sink during the period January–April. Their fluxes, as calculated with the relationship between the transfer velocity and the wind speed according to Tans et al. (1990), are similar to the model results for this area (-0.019 GtonC/period and -0.020 Gton C/period respectively). For the Atlantic and Indian ocean sectors in austral summer, Robertson and Watson (1995) and Poisson et al. (1994), using the relationship between transfer velocity and wind speed of Wanninkhof (1992), calculated CO_2 fluxes which are close to the model estimates (-0.10 Gton C/period vs -0.08 Gton C/period in the Atlantic sector and same value -0.016 Gton C/period in the Indian sector). Thus for several areas in the spring/summer period where CO_2 fluxes derived from field observations were available, the calculated fluxes obtained from our model appeared to be close to reality. This result suggests that the satellite-derived wind speeds better represent real-

ity than the climatological ones for the southern ocean. The wind speed data from which the climatologies are derived are rather sparse and probably not representative of climatological features, particularly in winter period.

3. Comparison between modelled and observed fCO_2

As the air–sea CO_2 fluxes depend both on the CO_2 exchange coefficient and on the air–sea fCO_2 gradient (ΔfCO_2), correctly calculated fluxes do not automatically mean that the simulated fCO_2 fields by the model are correct. As a means to improve the CO_2 flux estimate for the southern ocean, the differences between observed and modelled surface ocean fCO_2 are analyzed. Data from several cruises in the southern ocean were used (Table 1), the tracks of which are depicted in Fig. 2. To compare the model results with the observations, the data were averaged on the model grid of 2° latitude by 2° longitude, and standardized to an atmospheric pressure of 1013 hPa (used in the model). A change of 10 hPa in atmospheric pressure induces an effect of about 4 μatm in oceanic fCO_2. The air–sea CO_2 fluxes are calculated from observations with the atmospheric CO_2 concentration, the atmospheric pressure and the wind-speeds used in the model. The model results are extracted for the grid points over the periods for which observational data are available.

We investigated the differences between modelled and observed fCO_2 in several areas: the Kerguelen plateau, the boundaries of the Indian sector, the Eastern Pacific sector and the Atlantic sector with the Weddell gyre (refer to Fig. 2). On each track the model results are extracted in terms of fCO_2 and air–sea CO_2 fluxes and compared to the corresponding observations. The comparison track by track is described below.

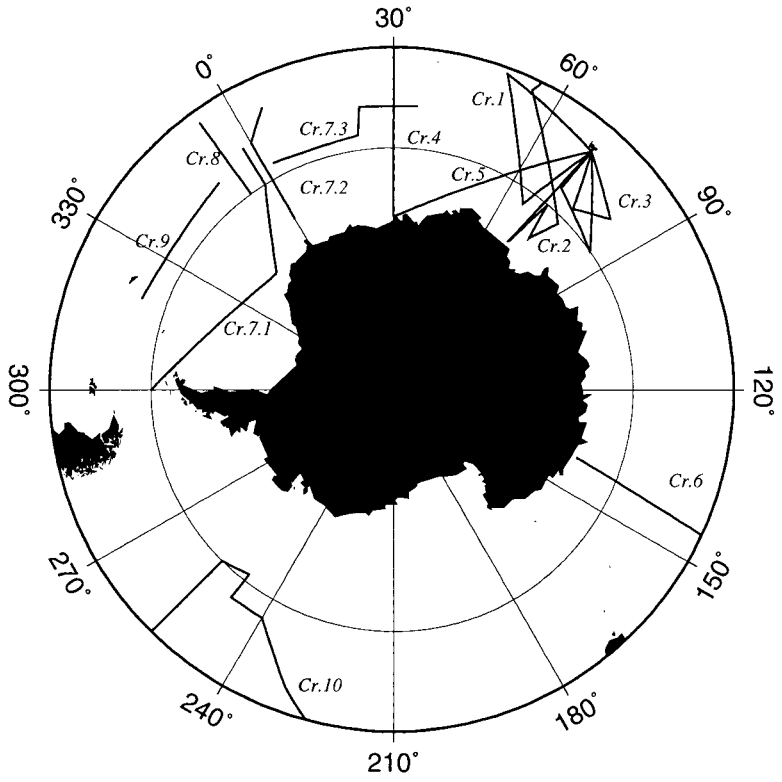

Fig. 2. Cruise tracks from which fCO_2 data were used in the southern ocean. Tracks 1–6 are cruises in the Indian sector, 7–9 in the Atlantic sector and 10 in the Pacific sector.

Table 1. *Summary of the averaged differences between the modelled and the actually observed fCO_2 in the surface layer and the air–sea CO_2 fluxes calculated from this for several cruises in the southern ocean; also given are the corresponding differences in temperature and salinity of the surface layer. The summary for each sector includes an estimate of the air–sea CO2 fluxes difference in GtC integrated over specified area and period. Cruise numbers correspond to the numbers in Fig. 2*

Cruise	Period	Region	Refs	δTemperature (°C)	δSalinity	δfCO_2 (μatm)	F_{CO_2} "obs" (mmol m^2 d^{-1})	F_{CO_2} mod (mmol m^2 d^{-1})	δF_{CO_2} (mmol m^2 d^{-1})
1	Jan.–Feb. 1991	Kerguelen plateau	Poisson et al. (1994)	−0.49	−0.005	−2.1	−2.52	−2.68	−0.2
2	Feb.–March 1991	Kerguelen plateau	Poisson et al. (1994)	+0.35	+0.050	+0.6	−0.72	−0.50	+0.2
3	April–May 1993	Kerguelen plateau	Louanchi (1995)	−0.40	−0.330	−8.4	+0.88	−2.20	−3.1
4	Feb. 1993	Along 30°E	Poisson et al. (1994)	−0.11	−0.130	−13.5	−2.83	−5.34	−2.5
5	Feb. 1993	Kerguelen–Antarctica 30°E	Poisson et al. (1994)	+0.24	−0.190	−8.0	−2.55	−2.78	−0.2
6	Feb. 1997	Along 143°E	Metzl et al. (1997)	−1.20	+0.120	+3.7	+1.26	+2.01	+0.7
7	March–May 1996	Weddell gyre, prime meridian	Stoll et al. (1997)	−0.18	−0.040	−37.5	+1.31	−8.13	−9.4
8	Oct.–Nov. 1992	Along 6°W, 47–60°S	Bakker et al. (1997)	+1.94	+0.220	−60.6	+4.88	−7.06	−11.9
9	Oct. 1992	Along 56–58°S	Bakker et al. (subm.)	+0.13	+0.001	−40.0	+0.14	−16.30	−16.4
10	March 1989	Along 105°W and 120–130°W	Murphy et al. (1991)	+0.16	+0.004	+9.7	−2.16	+0.67	+3.8
		Indian Sector (20–150°E)		−0.14	−0.064	−4.5	−1.07	−2.03	−0.9
	Jan. to Apr.	10.0 10^6 km^2 (ice free)							(−0.013 GtC)
		Pacific Sector (150°E–70°W)		+0.16	+0.004	+9.7	−2.16	+0.67	+3.8
	March	15.7 10^6 km^2 (ice free)							(+0.022 GtC)
		Atlantic Sector (70°W–20°E)		+0.34	+0.022	−43.6	+16	−10.06	−11.2
	Apr. to Nov.	7.01 10^6 km^2 (ice free)							(−0.230 GtC)

3.1. Kerguelen plateau

Fig. 3 shows the modelled and observed fCO_2 in the area of the Kerguelen plateau. This region is characterized by high spatio-temporal variability both in ocean dynamics and in biological processes. The model simulates quite well the mosaic of potential CO_2 sources and sinks as previously described (Poisson et al., 1994). It represents also the observed large-scale north–south features. However, in a few cases differences between modelled and observed fCO_2 of up to 20 µatm are found. These differences are generally observed for the area near Kerguelen Island (around 50°S) where specific coastal processes occur and are not described by the model.

In January–February 1991 (Fig. 3a) the observations show a mosaic of CO_2 sources and sinks. This is related to the intensive topography-circulation interactions by the Kerguelen plateau. The model underestimates both fCO_2 (Fig. 3a) and the SST (Fig. 3b). The difference in SST can explain most of the discrepancy between observed and modelled fCO_2. For SST higher than 4°C, the observed salinity is lower and the observed SST is higher than in the model (imposed by the constraints). This implies that in that area the observed hydrographic parameters indicate that less mixing of subsurface waters occurred than induced by the model constraints. In the northern part of the track the modelled and observed fCO_2 are nearly equal, indicating that the overestimated effect of mixing on the modelled fCO_2 is largely cancelled out by the lower SST. The model underestimates fCO_2 by 2.1 µatm on average, leading to an overestimation of the sink by 0.2 mmol $m^{-2}\,d^{-1}$ (Table 1).

In February–March 1991 (Fig. 3c), the model slightly overestimates the observed fCO_2 by 0.6 µatm leading to an underestimation of the sink by 0.2 mmol $m^{-2}\,d^{-1}$ (Table 1). The mean SST is higher by 0.35°C in the model than in the observations (Fig. 3d). This temperature difference would lead to an underestimation of fCO_2 of 5 µatm. However, the salinity appears to be higher in the

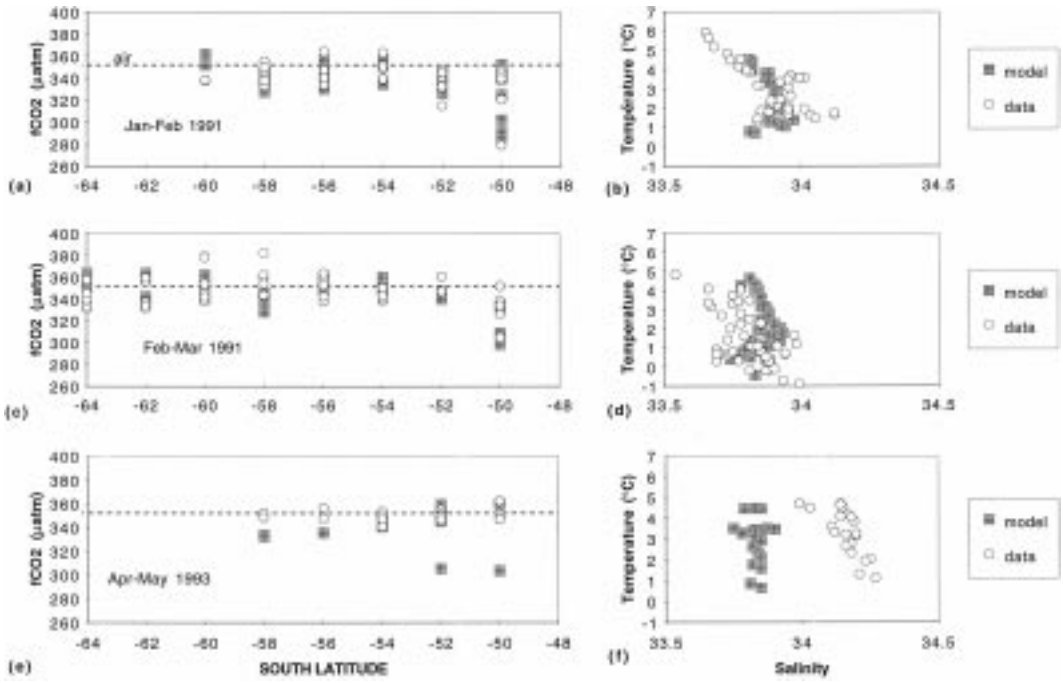

Fig. 3. Distribution of observed (circles) and modelled (cross shadowed) fCO_2 values (a,c,e) with the corresponding surface water temperature/salinity diagrams (b,d,f) for tracks 1, 2 and 3, respectively (refer to Fig. 2) in the area of the Kerguelen plateau. On each latitude, several data appear. Note that the high spatial variability of observed fCO_2 is well reproduced by the model.

model constraints than in the observations, possibly indicating that mixing of subsurface waters may in reality be more important than in the model. The enhanced effect of mixing, tending to increase the fCO_2, may have compensated the observed temperature difference.

In April–May 1993 (Fig. 3e) the in situ observations revealed that the ocean was nearly in equilibrium with the atmosphere with respect to CO_2. The model results and the observations in this area agree well, except for the region around Kerguelen Island where the model underestimates fCO_2 by more than 40 μatm. Half of this discrepancy is due to the temperature used as constraints of the model (Fig. 3f), which is lower than the observed temperature by more than 1°C. The in situ observed salinity is much higher in autumn (Fig. 3f) than in summer (Fig. 3b,d). This implies that intensive mixing has occurred (which at the same time leads to a temperature decrease on a seasonal scale), tending to increase the fCO_2. The salinity constraints in the model still represent summer conditions. Hence the mixing effect which depends on salinity profiles (see Section 7) is underestimated by the model in this period. In conclusion, the modelled fCO_2 in the Kerguelen plateau region is underestimated by 8.4 μatm leading to an overestimate of the sink by 3.1 mmol $m^{-2} d^{-1}$.

3.2. *Eastern and western boundaries of the Indian sector*

In February 1993 in the western Indian sector (Fig. 4a,c), the in situ observations show that different regimes in fCO_2 distribution can be distinguished: In the south the oceanic fCO_2 is supersaturated which is linked to the occurrence of the Antarctic Divergence (AD) where CO_2-enriched subsurface water is transported into the surface layer (Poisson et al., 1994). North of the AD the fCO_2 is undersaturated with values around 330 μatm (Fig. 4a,c). On track 5 (see Table 1), the model overestimates fCO_2 in the northern part of the area (between 52°S and 60°S) and underestimates fCO_2 south of 62°S. This is mainly due to different thermodynamical conditions in the in situ observations and climatological model constraints (Fig. 4d). As based on observed hydrological and geochemical properties during CIVA1/WOCE cruise, the AD signal is located around 64–66°S. By contrast, the model by its constraints produces an AD signal around 60°S. The mean difference in fCO_2 due to this inconsistency is about 10 μatm, leading to an overestimation of the sink by 2 mmol $m^{-2} d^{-1}$ in this area. If the modelled fCO_2 from the 60–50°S region is spatially translated to the 66–56°S region (represented by the dotted lines in Fig. 4a,c), then the agreement between the observations and the model improves significantly. The constraints being climatological properties, they smooth the physical structures in the area.

In February 1997, along the 143°E meridian (Fig. 4e), the observed and modelled fCO_2 data are in good agreement, both showing potential sources. However, the thermodynamical properties observed and those used in the model are rather different (Fig. 4f), the mean SST being lower and the salinity higher in the model than in reality. This implies that in the model the effect of mixing is too large (also see Table 1), which would lead to an overestimation of the fCO_2. On the other hand, correcting the model fCO_2 for the temperature indicates that the modelled fCO_2 may be too high by 15 μatm. Obviously the overestimation through mixing is largely compensated by the too low temperature in the model. Finally, on average the model slightly overestimates fCO_2 by 3.7 μatm leading to an overestimation of the CO_2 source by 0.6 mmol $m^{-2} d^{-1}$.

3.3. *Pacific sector*

Fig. 5 shows the modelled and observed fCO_2 along 2 tracks in the Pacific sector. The first track is along 125–130W (Fig. 5a,b), and the second track is along 105°W (Fig. 5c,d). There is generally a good agreement between hydrographic parameters used in the model and the observed ones (Fig. 5b,d). As a result the differences between modelled and observed fCO_2 are small on both tracks except in the area of the polar front around 50°S and the Antarctic divergence area around 60°S (Fig. 5a). Along 125°W, both modelled and observed fCO_2 are close to the atmospheric CO_2 level between 52 and 58°S. Whereas along 105°W, the surface layer appears to be undersaturated by −30 μatm on the same zonal band (Fig. 5c). Along 125–130°W, the model overestimates fCO_2 by 12.2 μatm leading to a difference of 3.6 mmol $m^{-2} d^{-1}$ in air–sea CO_2 flux. This discrepancy

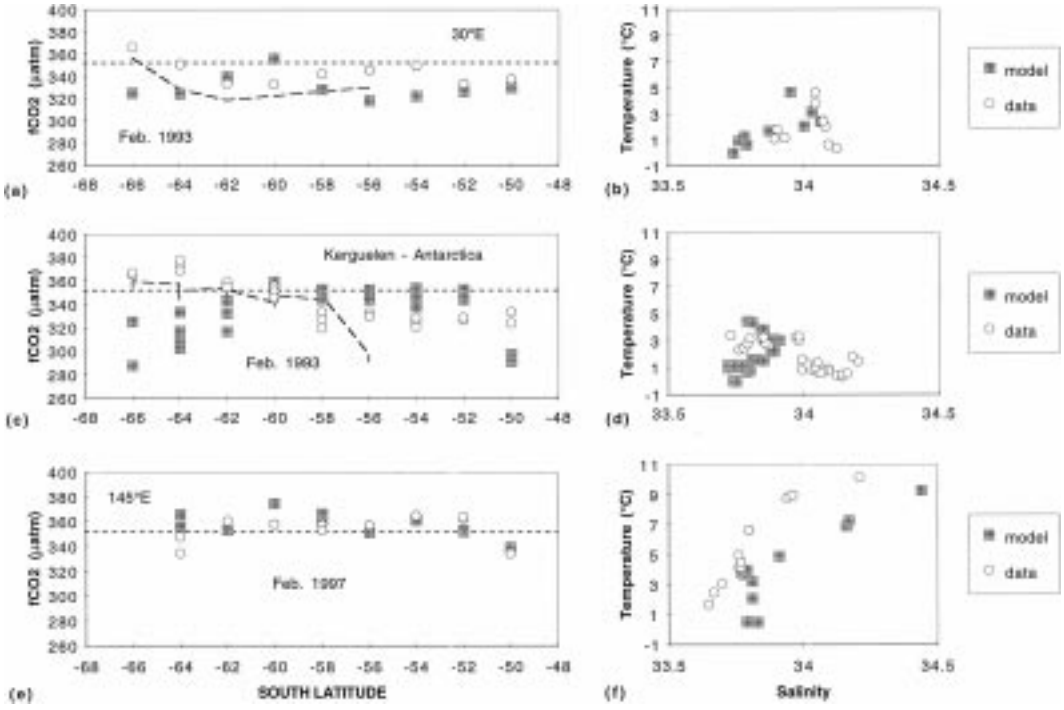

Fig. 4. Distribution of observed (circles) and modelled (cross shadowed) fCO_2 values (a,c,e) with the corresponding surface water temperature/salinity diagrams (b,d,f) for tracks 4 (along 30°E), 5 (Kerguelen–Antarctica at 30°E) and 6 (along 143°E), respectively (Fig. 2). During CIVA 1 cruise, the Antarctic Divergence (AD) was identified around 65°S from hydrographic and geochemical parameters. Levitus 94 temperature and salinity climatologies give this signal around 60°S. The dashed line represents modelled fCO_2 distribution if no mismatch in AD position was found.

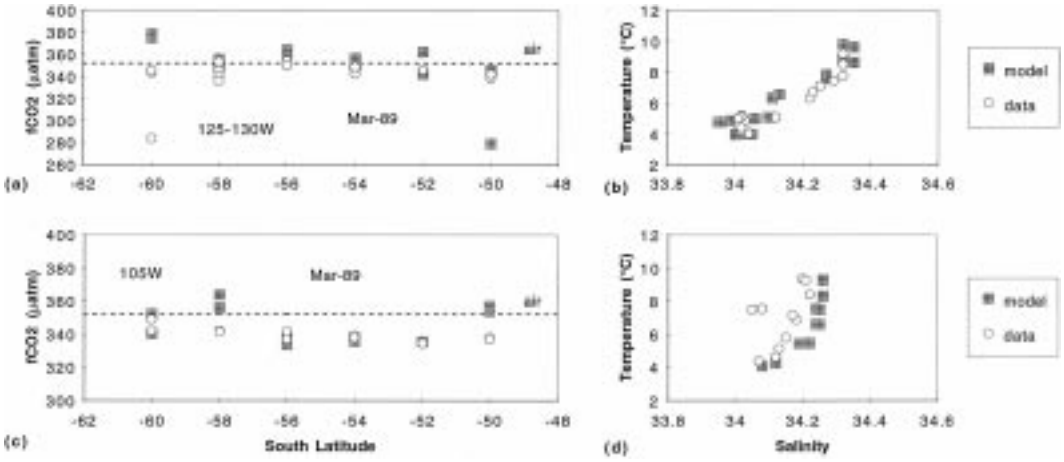

Fig. 5. Distribution of observed (circles) and modelled (cross shadowed) fCO_2 values (a,c) with the corresponding surface water temperature/salinity diagrams (b,d) for tracks 10 in the Pacific sector of the southern ocean along 120–130°W and 105°W, respectively (refer to Fig. 2). Note that the model reproduces the observed spatial variation of fCO_2 on the same zonal band.

leads to the conversion of the area from an observed sink of 2 mmol $m^{-2} d^{-1}$ into a source of 1.5 mmol $m^{-2} d^{-1}$. However, this difference between model and observations is largely due to temperature differences (Table 1). Applying a temperature correction (according to the polynomial of Goyet et al., 1993), the discrepancy is decreased to 4.2 µatm. The mixing conditions are similar between model and observations as indicated by similar averaged salinities (Fig. 5b).

Along 105°W, the difference between observed and modelled fCO_2 is less with a value of 5.8 µatm (Fig. 5c). The model slightly overestimates fCO_2, leading to an underestimation of the CO_2 sink on that track by 1.5 mmol $m^{-2} d^{-1}$ (-2.3 mmol $m^{-2} d^{-1}$ for the observed fluxes versus -0.7 mmol $m^{-2} d^{-1}$ for the modelled ones). On this track, temperature is not responsible for the discrepancy (Table 1). From salinity (Fig. 5d), it appears that the stratification was more important during the cruise than induced by the climatologies for this period. Thus, the mixing conditions in the model imply higher fCO_2, whereas the data show typical late summer conditions.

Finally, the difference between data and model on average in the cruise area is 9.2 µatm for fCO_2 (6.0 µatm when applying the temperature correction) leading to the conversion of the observed CO_2 sink of -2.2 mmol $m^{-2} d^{-1}$ into a small source of 0.7 mmol $m^{-2} d^{-1}$ (Table 1).

3.4. *Atlantic sector with Weddell gyre*

Fig. 6 shows the modelled and observed fCO_2 along the tracks in the Atlantic sector. Large underestimations appear in the model results compared to the observations for both the early spring and early winter periods.

In March–May 1996 (Fig. 6a), discrepancies of up to 100 µatm are found, but in the northern part the underestimates do not exceed 30 µatm. The accompanying SST/salinity diagram (Fig. 6b) shows that the constraints used in the model are in good agreement with the in situ data for SST larger than 0°C. Under the ice (SST -1.8°C) the salinities in the model are underestimated (Fig. 6b), indicating less intensive admixture of subsurface waters in the model than in reality. Different mixing conditions can only partly explain the large discrepancy between the modelled and observed fCO_2. As the low fCO_2 values produced by the model are related to a relatively high biological activity in this area at this period (calculated by means of satellite-derived chlorophyll), the effect of biological activity on the fCO_2 is probably overestimated through these model constraints. The mean underestimation of fCO_2 by the model amounts to 37.5 µatm for this area, leading to an overestimation of the CO_2 uptake by 9.4 mmol $m^{-2} d^{-1}$ (Table 1).

Along the 6°W meridian in October–November 1992 (Fig. 6c), the in situ observations show that south of 50°S the ocean was supersaturated in CO_2 most of the time. In austral spring the retreat of the sea ice is followed by an increase of the sea surface temperature which induces an increase of the fCO_2 and a possible supersaturation. The model does not reproduce this feature (Fig. 6c). During the cruise the biological activity was low south of the polar frontal zone (Bakker et al., 1997), and the ice limit was found around 56°S. In the model constraints, the ice limit is defined near 60°S for this period, favouring the development of blooms in the area between 54°S and 60°S because biological activity in the model also depends on the ice cover (see Section 7). In fact, the observational fCO_2 data show late winter conditions, whereas the model simulates spring conditions for that track. Note that the SST/salinity diagram shows a good agreement between model and in situ observations (Fig. 6d), which suggests that the mixing conditions were satisfactorily simulated by the model. The discrepancy between modelled and observed fCO_2 thus arises primarily from differences in biological cycle stages.

Along 56–58°S latitude in October 1992 (Fig. 6e) the zonal differences between model and observations decrease eastward. The accompanying SST/salinity diagram (Fig. 6f) discloses that the hydrographic conditions definitely do not describe the real situation. During this period, the melting of the sea ice was just starting (Bakker, 1998). By contrast, the model simulates spring conditions with a low percentage of ice coverage and the beginning of stratification favouring phytoplankton blooms. Deviations both of the physical and biological description of the sea surface layer are responsible for the low level of the fCO_2 in the model results. The mean fCO_2 difference of -60.6 µatm between model and observations induces an overestimation of the sink

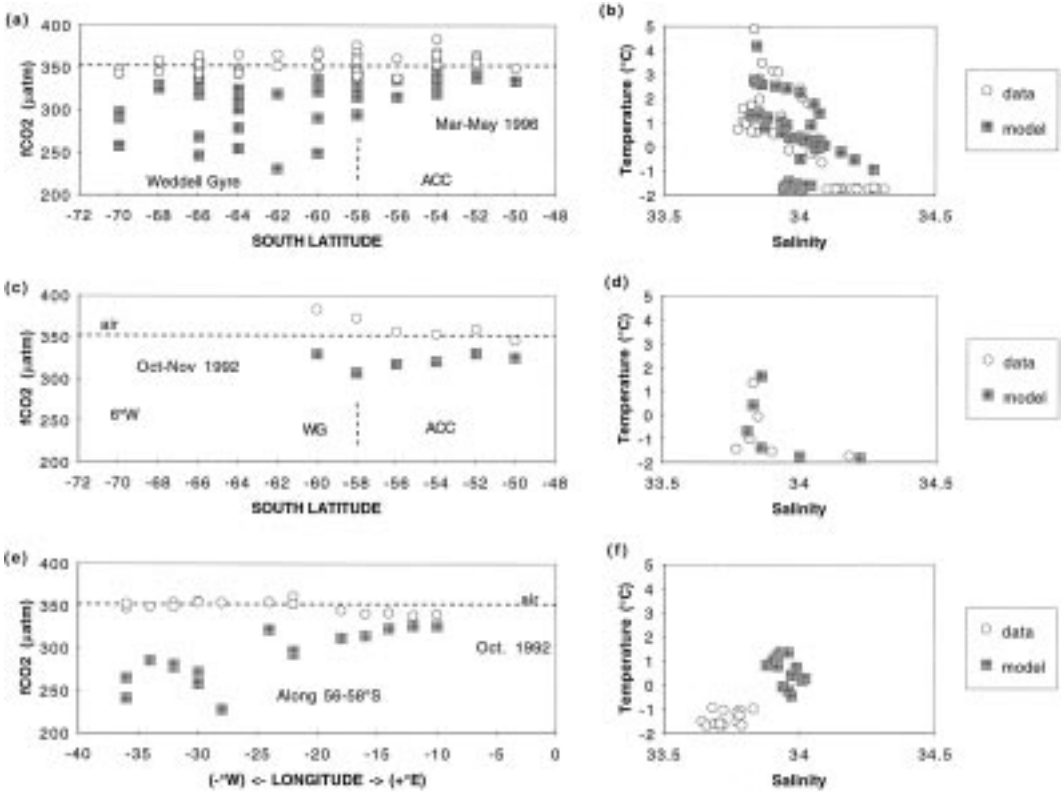

Fig. 6. Distribution of observed (circles) and modelled (cross shadowed) fCO_2 values (a,c,e) with the corresponding surface water temperature/salinity diagrams (b,d,f) for tracks 7 (Atlantic sector/Weddell gyre), 8 (56–58°S latitude) and 9 (along 6°W), respectively (refer to Fig. 2). Note the decrease of the differences between modelled and observed fCO_2 northward and eastward.

produced by the model by -16.4 mmol m^{-2} d^{-1} (Table 1). Overall, the model underestimates the fCO_2 in the Atlantic sector by 43 µatm on average, leading to an overestimation of the CO_2 sink of the Atlantic sector by 11 mmol m^{-2} d^{-1} for the early spring and the early winter periods. These discrepancies cannot be extrapolated to the Indian sector since the differences between model and data are decreasing eastward.

The mean differences between observed and modelled fCO_2 are presented in Table 1 for the entire southern ocean. For the Indian sector of the southern ocean the model underestimates the fCO_2 by only 4 µatm which is equal to an overestimation of the CO_2 uptake calculated by the model of 0.01 GtC for the January–April period (Table 1). This diffence is small compared to the uptake originally calculated by the model for that sector (0.23 GtC yr^{-1}), indicating that the model can satisfactorily be applied to this region. This can also be concluded for the Pacific sector where the difference between modelled and observed fCO_2 leads to a small underestimation of CO_2 sink by 0.02 GtC in March. For the Atlantic sector of the southern ocean the mean difference between modelled and observed fCO_2 is as high as -43.6 µatm from which an overestimation of the CO_2 uptake by 0.23 GtC for the April to November period can be calculated. The total uptake modelled for the Atlantic sector of 0.47 GtC yr^{-1} would have to be reduced by 50% to reproduce the observed fluxes.

More generally, when comparing the results of the recent climatology of Takahashi et al. (1997) to the model results in terms of air–sea CO_2 gradient ΔfCO_2 annual average, the model gives

−9.5 μatm and −8.4 μatm for the Pacific and Indian sectors respectively. These values are very close to the −7.9 μatm estimated by Takahashi et al. (1997) for the whole southern ocean south of 50°S. On the contrary, the Atlantic sector sink is highly overestimated with an average value of −28.5 μatm for the annual ΔfCO_2. Such a large undersaturation may not be surprising for this area in the summer period when a relatively high primary production occurs (compared to other areas of the southern ocean), but this is certainly not the case for the winter period as demonstrated by this comparative study.

4. Sensitivity analysis

As the main uncertainty regarding the CO_2 uptake originates from the Atlantic region, a sensitivity analysis was performed to assess the impact of the physical constraints on the air–sea CO_2 exchange in this region. It should be realized that the constraints fields used in the model are derived from climatological data including early observations, which indirectly introduces a large uncertainty in air–sea CO_2 fluxes (Section 3). In addition, the amount of data for the southern ocean in such data bases is relatively small, particularly for the winter period under the ice. Only when more observational data become available can the performance of the diagnostic model of fCO_2 be improved. The only data bases available at a reasonable space and time grid are those of Levitus and Boyer (1994) and Levitus et al. (1994). Most of the modelling studies currently use these data even when for some periods and some areas statistical extrapolations were performed in these data bases.

The effects of upwelling velocity, the mixed-layer depth (MLD) and the ice coverage are now discussed. In the standard analysis, the upwelling velocity was taken to be 45 m yr^{-1} as reported by Gordon and Huber (1990). However, in certain areas the upwelling velocity may reach much higher values (Gargett, 1991). Fig. 7a shows the monthly average of the MLD derived from Levitus (1994) as used in the model. However, the MLD cycle derived from the constraints fields does neither exactly agree with the observations nor with our knowledge of the southern ocean (long

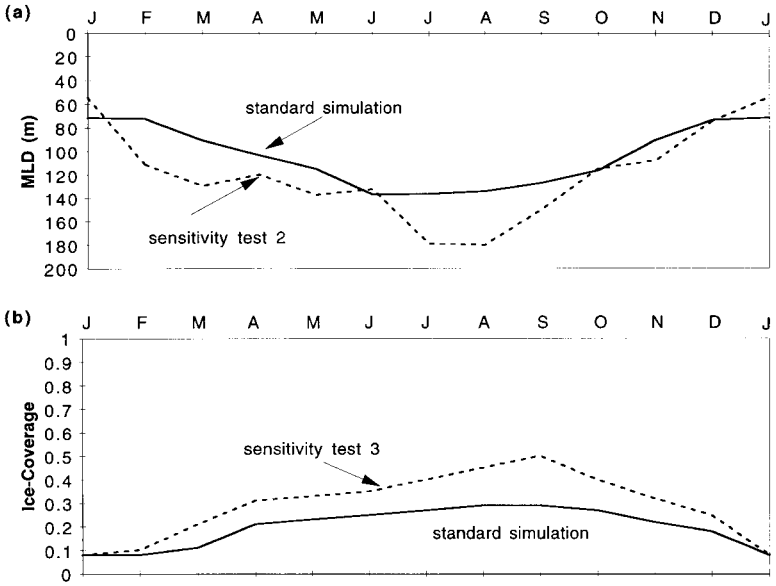

Fig. 7. Monthly averages of the mixed-layer depth (a) and the ice coverage (b) used as constraints in the modelling study in the Atlantic sector of the southern ocean (black line). The dotted line represents the same constraints which are derived from the observed SST and satellite-derived wind speeds fields changes and used for the sensitivity analysis. Both mixed-layer depth and ice coverage used in the standard simulation show a smooth seasonal signal.

winter period of 9 months and short spring–summer period of 3 months for the seasonal ice zone, SIZ). Typical examples of this are that the depth of the mixed-layer does not exceed 135 m for the June–August period and the spring conditions start in September–October. In addition, differences in the ice limit and hence in the SIZ definition were noticed between the observations and the model constraints for the early winter and early spring. Fig. 7b represents the monthly average of the percentage ice coverage. In Fig. 7a,b the dotted line represents the conditions used for the sensitivity tests.

The results of five simulations are presented in Table 2 in terms of annual mean ΔfCO_2 and annual CO_2 uptake. The standard simulation results in a mean ΔfCO_2 of -28.5 μatm for the whole Atlantic sector inducing a CO_2 uptake of 0.47 GtC yr^{-1}. If the upwelling velocity is increased from 45 m yr^{-1} (standard run) to 90 m yr^{-1} for the whole area, the ΔfCO_2 is reduced by about 30% and the CO_2 uptake by 25%. Changing the MLD according to Fig. 7a leads to a reduction of 40% in ΔfCO_2 and of 45% for the CO_2 uptake. Changing the ice coverage according to Fig. 7b does not affect ΔfCO_2 but the CO_2 uptake is reduced by 20% because less surface is available. If all these effects are taken into account the ΔfCO_2 and the CO_2 uptake are reduced by more than 60%. Thus, the CO_2 uptake by the southern ocean is very sensitive to the changes in these dynamical properties. These changes are also sensitive to variations of climatic conditions. For example, in a colder year the SST is relatively low which affects the distribution of the fCO_2 but also affects the ice coverage. The impact on the air–sea fluxes can be either less uptake because of the surface area for air–sea exchange is reduced, or more uptake because the SST decreases the fCO_2. Moreover, in a colder year the mean wind speed is generally elevated, which promotes more air–sea exchange of CO_2 but also more mixing of CO_2-rich subsurface water. It should be added that such deliberations are particularly relevant for the southern ocean because the largest CO_2 exchange coefficients (deduced from satellite-derived wind speeds) are found in this region (Boutin and Etcheto, 1997).

In summary, the uncertainties in the CO_2 uptake of the southern ocean are mainly due to the lack of observational data and to the lack of an accurate knowledge of the seasonal variation of circulation features in that area. More measurements and a better representation of the SIZ processes in the model would help to improve the quantification of the southern ocean CO_2 sink.

Table 2. *Results of the sensitivity tests for the model results of the Weddell gyre and its impact on the air–sea CO_2 flux; the change in mixed-layer depth and ice cover were done according to Fig. 7; the simulation "all together" calculates the result when all three sensitivity tests are applied at the same time; for more details, see text*

Simulations	Test no.	ΔfCO_2 (μatm)	ΔCO_2 flux (Gt C yr^{-1})
standard	0	−28.5	−0.47
$Kz = 90$ m yr^{-1}	1	−20.4	−0.35
change MLD	2	−17.3	−0.29
change ice cover	3	−26.9	−0.37
all together	4	−11.9	−0.18

5. Conclusions

This comparative study shows that our model reproduces well the zonal and meridional distributions and the seasonal signal in the Indian and Pacific sectors of the southern ocean. On the other hand, large discrepancies between modelled and observed fCO_2 are found in the Atlantic sector mostly due to the constraints used in the model, translating into a difference in the annual CO_2 uptake by the Atlantic sector of 0.2–0.3 GtC yr^{-1}. However, this difference in annual uptake was calculated, presuming that the seasonal cycle in the model and in reality are exactly identical. This implies that any difference between modelled and observed fCO_2 counts to the full extent. However, there may also exist a temporal shift in the seasonal cycles of the model results and the in situ observations. In this case the same levels of fCO_2 could be reached in the model and in reality but in a different stage of the season. This would result in a much smaller calculated difference in the annual CO_2 uptake than the 0.2–0.3 GtC yr^{-1} calculated above. A shift, or more generally, a difference in the seasonal cycles of the model and the real ocean is not unlikely as interannual differences in carbon cycling do undoubtedly

occur. Note that in our discussion in Section 3 seasonal shifts were invoked to explain specific results. Also in our previous study with the model (unpublished results) seasonal shifts in the simulation of dissolved inorganic carbon in the Weddell gyre were discerned, where in light of the present discussion the important outcome was that the seasonal amplitude of variations was correctly simulated. As indeed the model is based on monthly variations of the constraints which are climatologies of observed fields, the seasonal signal (the seasonal amplitude) is generally well reproduced. It is the lack of information in the seasonal ice zone which means that just in this area the absolute value of fCO_2 is underestimated. It is worth adding that the fCO_2 tracks in the Atlantic sector, that were used to validate the model (Table 1), originate from seasons (tracks 8 and 9: early spring; track 7: beginning of the winter) in which the physical conditions in the ocean were in a state of changing. This contrasts with the tracks in the Indian or the Pacific sectors, which originate from more or less stable summer conditions (Table 1). Thus, it is not surprising that, if differences exist in the seasonal cycles of the model and the real ocean, these would become visible in the Atlantic sector. In conclusion, the large difference between the modelled and observed fCO_2 in the Weddell gyre is admittedly alarming, but as this may be explained by a seasonal shift this makes the mismatch in fluxes much less dramatic.

Thus, the model estimate for the annual CO_2 uptake of the southern ocean has to be moderated for the Weddell gyre by 0.2–0.3 GtC at most, leading to an uptake of 0.2 GtC yr^{-1} as a lower boundary for latter area against 0.47 GtC yr^{-1} for our earlier estimate (Section 2). By contrast, in the Indian sector the model reproduces quite well the observed signal in summer, mostly because of a better representation of the mixing conditions in the constraints fields. A striking result is the good simulation of the high variability in fCO_2 encountered in the area of the Kerguelen plateau (in the Indian sector). This puts confidence in our approach using this diagnostic model for fCO_2, provided the physical constraints on the model are reliable. Moreover, the ability of the model to reproduce a correct fCO_2 signal in the Pacific sector is very encouraging since the model is highly dependent on the definition of subsurface parameters, and except the GEOSECS data, we had no more cruises for defining DIC and TA in that sector (Section 2). Extrapolating monthly fCO_2 fields over large areas by using the changes in climatological constraints may be a powerful tool to successfully estimate the global oceanic CO_2 uptake.

The model estimate for the total CO_2 uptake of the southern ocean of 0.9 GtC yr^{-1} has to be corrected for the discrepancy in the Atlantic sector. A more realistic estimate is 0.6–0.7 GtC yr^{-1}. It is worth noting that this value approaches the one from Tans et al. (1990) as reestimated by using satellite-derived wind-speeds instead of climatological ones (Section 2). The range of the new estimate is introduced due to the seasonal incongruency of the model and the real ocean. Albeit we verified our earlier estimation, some uncertainty remains, which is mainly due to the lack of winter data particularly in the seasonal ice zone.

Interannual variations in climatic conditions and hence in the constraints of the sea surface CO_2 system strongly affect the oceanic CO_2 uptake as demonstrated in this study. Francey et al. (1995) and Keeling et al. (1995) have also shown that the interannual climate variations strongly affect the global carbon budget. Lévy (1996) demonstrated that the mesoscale variability of the dynamic structure of the ocean may lead to an underestimation of the primary production and hence to uncertainty in the mesoscale fCO_2 distribution. These spatio-temporal variabilities may induce large uncertainties in the carbon budget. As our model uses monthly climatological constraints, it is obviously unable to reproduce such local and time-specific signals in the fCO_2 distribution.

One way to progress is to relate the MLD changes to changes in wind speed and SST (which are available from satellite at weekly and interannual scales), or to use MLD values from realistic general circulation models. Unfortunately, there are still some uncertainties in describing the oceanic circulation in the OGCMs, particularly for the southern ocean (Orr et al., 1997), and more data are necessary to better constrain the models at global and regional scale. A better representation of the sea surface fCO_2 spatio-temporal variability will give better constraints on atmospheric models and hence on the global carbon budget.

6. Acknowledgements

We thank Dr. Jacqueline Boutin and Dr. Jacqueline Etcheto (LODYC, Paris) for providing the satellite-derived wind-speed fields. Dr. Nicolas Metzl (LPCM, Paris) is acknowledged for the data processing of the Tasmania-Antarctic cruise in 1997. We thank the captains and crews of the RV *Polarstern* and *Marion-Dufresne* for their continuous help on board. This work was supported by the PROCOPE program of cooperation between AWI Bremerhaven and LPCM Paris, and the "JGOFS-France Modélisation" program. Dr. Raymond G. Najjar and Prof. Andrew J. Watson are acknowledged for their comments on an earlier version of the manuscript. We are grateful to two anonymous reviewers for their constructive criticisms on this study.

7. Appendix

The one-dimensional diagnostic model of sea surface fCO_2 is based on the translation of variations in monthly constraints into fCO_2 variations. The main processes controlling sea surface fCO_2 variations are estimated at each time step as a function of the variations of the constraints. These physical and biogeochemical processes are: the air–sea exchange, the mixing effect, the thermodynamics of the carbonate system and the biological uptake and release. Each process affects DIC, TA and TIN the three state variables of the model. The effects on fCO_2 changes are computed at each time step from DIC, TA, temperature and salinity.

7.1. *Air–sea exchange effect*

The air–sea exchange of CO_2 is calculated according to Wanninkhof (1992). At each time step the flux at the air–sea interface (F_{CO_2}) is calculated as a function of the wind speed, the temperature and the salinity and translated into a change of dissolved inorganic carbon:

$$F_{CO_2} = (1-g)KS_{CO_2}\Delta fCO_2,$$

where g is the ice coverage, K the piston velocity, S_{CO_2} is the CO_2 solubility and ΔfCO_2 the air–sea fCO_2 difference. The air–sea exchange affects only DIC in the mixed-layer depth and the variations of the latter according to this process is computed at each time-step as follows:

$$\delta\mathrm{DIC} = F_{CO_2}\,\delta t/Z,$$

where Z is the mixed-layer depth.

7.2. *Mixing effect*

The mixing effect is estimated as the entrainment/detrainment effect described in Peng et al. (1987) as well as through the input of subsurface properties into the surface layer by the general southern ocean upwelling. These processes affect inorganic nitrogen, alkalinity and dissolved inorganic carbon and are dependent on the mixed-layer depth and the surface–subsurface gradient of the geochemical properties. The subsurface properties are maintained constant during the whole year of simulation. Changes due to the mixing effect are calculated according to:

$$\delta G/\delta t = \delta Z/\delta t(G_b - G_s)/Z + Kz(G_b - G_s)/Z,$$

where G is the geochemical property, G_b and G_s are the concentrations of G in the subsurface and surface boxes, respectively, Z is the mixed-layer depth and Kz is the upwelling velocity.

7.3. *Biological effect*

Most of the parameterizations of the biological effect on fCO_2 are adapted from Taylor et al. (1991).

7.3.1. Net primary production. The variation of chlorophyll biomass is expressed as:

$$\delta\mathrm{Chl}/\delta t = (U-Q)\mathrm{Chl},$$

U is the growth of the phytoplankton and is expressed as a Michaelis–Menten function of the nutrient total inorganic nitrogen (TIN):

$$U = (1-g)U_m\mathrm{TIN}/(\mathrm{TIN} + K_m).$$

In this expression U_m is the maximal growth rate and K_m the half-saturation constant of the growth on TIN. U is calculated at each time-step also as a function of the ice coverage g. If $g = 1$, no growth of the phytoplankton can occur. Q represents the total loss of organic matter. It is deduced from U and Chl changes in the surface layer following the equation:

$$Q = U - \delta\ln(\mathrm{Chl})/\delta t.$$

Finally, the variation of TIN with time is:

$$\delta\mathrm{TIN}/\delta t = -(U - R_s Q)\mathrm{Chl\ N/Chl}.$$

In this expression, R_s represents the mineralization factor in the surface layer, N/Chl is the nitrogen to chlorophyll ratio in phytoplankton.

The maximal growth rate of the phytoplankton, $U_m = 1\ d^{-1}$, was obtained by means of sensitivity tests as the one which best represents the seasonal variation of DIC at several locations (unpublished). If U_m is increased to 2, the DIC level is reduced by 10 μmol/kg and the seasonal signal will be overestimated. In contrast, a smaller value of U_m ($0.5\ d^{-1}$) leads to a higher value of DIC and a smoothening of the seasonal signal. The model appears to be less sensitive to the upwelling rate as fCO_2 changes with less than 3 μatm for a 10 m/yr change. The removal factor R_s (factor of regeneration) is taken at 0.5 for the southern ocean according to Olson (1980) and Minas and Minas (1992).

7.3.2. Export production and $CaCO_3$ precipitation. The exported production is expressed in carbon units as:

$$P_{exp} = (1 - R_s)Q\ \mathrm{Chl\ C/Chl},$$

where C/Chl is the carbon to chlorophyll ratio in phytoplankton. We assume that 20% of the exported production consists of $CaCO_3$.

7.4. Estimating DIC and TA changes

Finally, the total variations of DIC and TA are:

$$\begin{aligned}\delta\mathrm{DIC}/\mathrm{d}t = {} & [(\delta TIN/\delta t)(C/N) - 0.2P_{exp}] \\ & + [\delta Z/\delta t(\mathrm{DIC_b} - \mathrm{DIC_s})/Z \\ & + Kz(\mathrm{DIC_b} - \mathrm{DIC_s})/Z] \\ & + [F_{CO_2}/Z],\end{aligned}$$

$$\begin{aligned}\delta\mathrm{TA}/\mathrm{d}t = {} & [-(\delta\mathrm{TIN}/\delta t)(1/1) - 2(0.2P_{exp})] \\ & + [\delta Z/\delta t(\mathrm{TA_b} - \mathrm{TA_s})/Z \\ & + \mathrm{Kz}(\mathrm{TA_b} - \mathrm{TA_s})/Z],\end{aligned}$$

where C/N is the Redfield ratio (Redfield et al., 1963). These variations are translated into fCO_2 variations using equilibrium constants of Goyet and Poisson (1989). The first term on the equations right represents the biological effect on DIC and TA variations, the second one represents the mixing effect, and the third one (only for DIC) the impact of the air–sea CO_2 exchange.

REFERENCES

Bainbridge, A. E. 1981. *Geosecs Atlantic expedition: hydrographic data*, vol. 1, 120 pp. US Government Printing Office, Washington, DC.

Bakker, D. C. E., De Baar, H. J. W. and Bathmann, U. V. 1997. Changes of carbon dioxide in surface waters during spring in the Southern Ocean. *Deep-Sea Res. II* **44**, 91–127.

Bakker, D. C. E. 1998. *Process studies of the air–sea exchange of carbon dioxide in the Atlantic Ocean.* PhD Thesis, Rijksuniveriteit Groningen, The Netherlands, 220 pp.

Boutin, J. and Etcheto, J. 1997. Long-term variability of the air–sea CO_2 exchange coefficient: Consequences for the CO_2 fluxes in the equatorial Pacific Ocean. *Global Biogeochem. Cycles* **11**, 453–470.

Broecker, W. S., Spencer, D. W. and Craig, H. 1982. *Geosecs Pacific expedition: hydrographic data*, vol. 3, 137 pp. US Government Printing Office, Washington, DC.

Ciais, P., Tans, P. P., Trolier, M., White, J. W. C. and Francey, R. J. 1995. A large northern hemisphere terrestrial CO_2 sink indicated by the $^{13}C/^{12}C$ ratio of atmospheric CO_2. *Science* **269**, 1098–1101.

Conway, T. J., Tans, P. P., Waterman, L. S., Thoning, K. W., Kitzis, D. R., Masarie, K. A. and Zhang, N. 1994. Evidence for interannual variability of the carbon cycle from the National Oceanic and Atmospheric Administration/Climate Monitoring and Diagnostics Laboratory global air sampling network. *J. Geophys. Res.* **D99**, 22831–22855.

Denning, A. S., Fung, I. Y. and Randall, D. 1995. Latitudinal gradient of atmospheric CO_2 due to seasonal exchange with land biota. *Nature* **376**, 240–243.

Francey, R. J., Tans, P. P., Allison, C. E., Enting, I. G., White, J. W. C. and Trolier, M. 1995. Changes in oceanic and terrestrial carbon uptake since 1982. *Nature* **373**, 326–330.

Gargett, A. E. 1991. Physical processes and the maintenance of nutrient-rich euphotic zones. *Limnol. Oceanogr.* **36**, 1527–1545.

Gloersen, P., Campbell, W. J., Cavalieri, D. J., Comiso, J. C., Parkinson, C. L. and Zwally, H. J. 1992. *Arctic and Antarctic sea ice, 1978–1987: satellite passive-microwave observations and analysis.* SP-511, Nat. Aeron. and Space Admin., Washington, DC.

Gordon, A. L. and Huber, B. A. 1990. Southern Ocean winter mixed layer. *J. Geophys. Res.* **C95**, 11655–11672.

Goyet, C. and Poisson, A. 1989. New determination of

carbonic acid dissociation constants in seawater as a function of temperature and salinity. *Deep-Sea Res.* **36**, 1635–1654.

Goyet, C., Millero, F. J., Poisson, A. and Shafer, D. K. 1993. Temperature dependance of CO_2 fugacity in seawater. *Mar. Chem.* **44**, 205–219.

Hoppema, M., Fahrbach, E., Schröder, M., Wisotzki, A. and De Baar, H. J. W. 1995. Winter–summer differences of carbon dioxide and oxygen in the Weddel Sea surface layer. *Mar. Chem.* **51**, 177–192.

Houghton, J. T., Meira Filho, L. G., Callander, B. A., Harris, N., Kattenberg, A. and Maskell, K. (eds.) 1996. *Climate change 1995 — The Science of Climate change: contribution of Working group I to the Second Assessment Report of the Intergovernmental Panel on Climate Change*. Cambridge University Press. Cambridge.

Keeling, C. D., Piper, S. C. and Heimann, M. 1989. A three-dimensional model of atmospheric CO_2 transport based on observed winds: 4. Mean annual gradients and interannual variations. In: *Aspects of Climate Variability in the Pacific and the Western Americas* (ed. D. H. Peterson). Geophys. Monogr. 55, AGU, Washington, DC, 305–363.

Keeling, C. D., Whorf, T. P., Wahlen, M. and Van der Plicht, J. 1995. Interannual extremes in the rate of rise of atmospheric carbon dioxide since 1980. *Nature* **375**, 666–670.

Keeling, R. F., Najjar, R. P., Bender, M. L. and Tans, P. P. 1993. What atmospheric oxygen measurements can tell us about the global carbon cycle. *Global Biogeochem. Cycles* **7**, 37–67.

Levitus S. and Boyer, T. P. 1994. *World Ocean Atlas 1994. Vol. 4: Temperature*. NOAA ATLAS NESDIS 4, 117 pp.

Levitus S., Burgett, R. and Boyer, T. P. 1994. *World Ocean Atlas 1994. Vol. 3: Salinity*. NOAA ATLAS NESDIS 3, 99 pp.

Lévy, M. 1996. *Modélisation des cycles biogéochimiques en Méditerranée nord-occidentale: variabilité mésoéchelle et cycle saisonnier*. Doctorat de l'Université Paris 6, PhD Thesis.

Louanchi, F. 1995. *Etude des variabilités spatio-temporelles de fCO_2 à la surface de l'océan Indien: Processus et quantification*. Doctorat de l'Université de Paris 6, PhD Thesis, 234 pp.

Louanchi, F., Metzl, N. and Poisson, A. 1996. Modelling the monthly sea surface fCO_2 fields in the Indian Ocean. *Mar. Chem.* **5**, 265–279.

Masarie, K. A. and Tans, P. P. 1995. Extension and integration of atmospheric carbon dioxide data into a globally consistent measurement record. *J. Geophys. Res.* **D100**, 11593–11610.

Metzl, N., Louanchi, F. and Poisson, A. 1999. Seasonal and interannual variations of sea surface carbon dioxide in the subtropical Indian Ocean. *Mar. Chem.*, **60**, 131–146.

Minas, H. J., and Minas, M. 1992. Net community production in "High Nutrient–Low Chlorophyll" waters of the tropical and Antarctic oceans: grazing vs. iron hypothesis. *Oceanol. Acta* **15**, 145–162.

Murphy, P. P., Feely, R. A., Gammon, R. H., Harrison, D. E., Kelly, K. C. and Waterman, L. S. 1991. Assessment of the air–sea exchange of CO_2 in the South Pacific during austral autumn. *J. Geophys. Res.* **C96**, 20455–20465.

Olson, R. J. 1980. Nitrate and ammonium uptake in Antarctic waters. *Limnol. Oceanogr.* **25**, 1064–1074.

Orr, J. C. 1996. The Ocean Carbon-Cycle Model Intercomparison Project of IGBP/GAIM. In: *Ocean storage of carbon dioxide* (ed. B. Ormerod). IEA Greenhouse Gas R&D Programme, 33–52.

Peng, T.-H, Takahashi, T., Broecker, W. S. and Olafsson, J. 1987. Seasonal variability of carbon dioxide, nutrients and oxygen in the northern North Atlantic surface water: observations and a model. *Tellus* **39B**, 439–458.

Poisson, A., Schauer, B. and Brunet, C. 1990. MD53/INDIGO 3. In: *Les rapports des campagnes à la mer, 87(02)*. Les publications de la Mission de Recherche des Terres Australes et Antarctiques Françaises, 269 pp., Paris.

Poisson, A., Metzl, N., Brunet, C., Schauer, B., Brès, B., Ruiz-Pino, D. and Louanchi, F. 1993. Variability of sources and sinks of CO_2 and in the western Indian and Southern Oceans during the year 1991. *J. Geophys. Res.* **C98**, 22759–22778.

Poisson, A., Metzl, N., Danet, X., Louanchi, F., Brunet, C., Schauer, B., Brès, B. and Ruiz-Pino, D. 1994. Air–sea CO_2 fluxes in the Southern Ocean between 25°E and 85°E. In: *The Polar oceans and their role in shaping the global environment* (eds. O. M. Johannessen et al.). Geophysical Monograph 85, AGU, Washington, DC, 273–284.

Redfield, A. C., Ketchum, B. H. and Richards, F. A. 1963. The influence of organisms on the composition of seawater. In: *The sea*, vol. 2 (ed. M. N. Hill). Wiley-Interscience, New York, 26–77.

Reynolds, R. W. and Marsico, D. C. 1993. An improved real-time global sea surface temperature analysis. *J. Climate* **6**, 114–119.

Robertson, J. E. and Watson, A. J. 1995. A summer-time sink for atmospheric carbon dioxide in the Southern Ocean between 88°W and 80°E. *Deep-Sea Res. II* **42**, 1081–1091.

Sarmiento, J. L., Orr, J. C. and Siegenthaler, U. 1992. A perturbation simulation model of CO_2 uptake in an ocean general circulation model. *J. Geophys. Res.* **C97**, 3621–3645.

Sarmiento, J. L. and Sundquist, E. T. 1992. Revised budget for the oceanic uptake of anthropogenic carbon dioxide. *Nature* **356**, 589–593.

Sarmiento, J. L. and Le Quéré, C. 1996. Oceanic carbon dioxide uptake in a model of century-scale global warming. *Science* **274**, 1346–1350.

Stoll, M. H. C., De Baar, H. J. W., Hoppema, M. and Fahrbach, E. 1998. Early winter pCO_2 data revealing

undersaturation in the fully ice covered Weddell Sea. *Mar. Chem.*, in press.

Takahashi, T., Olafsson, J., Goddard, J. G., Chipman, D. W. and Sutherland, S. C. 1993. Seasonal variation of CO_2 and nutrients in the high-latitude surface oceans: a comparative study. *Global Biogeochem. Cycles* **7**, 843–878.

Takahashi, T., Feely, R. A., Weiss, R. F., Wanninkhof, R. H., Chipman, D. W., Sutherland, S. C. and Takahashi, T. T. 1997. *Global air–sea flux of CO_2: an estimate based on measurements of air–sea pCO_2 difference*. Proc. Natl. Acad. Sci., Vol. 94, pp. 8292–8299, USA.

Tans, P. P., Fung, I. Y. and Takahashi, T. 1990. Observational constraints on the global atmospheric CO_2 budget. *Science* **247**, 1431–1438.

Tans, P. P., Berry, J. A. and Keeling, R. F. 1993. Oceanic $^{13}C/^{12}C$ observations: a new window on ocean CO_2 uptake. *Global Biogeochem. Cycles* **7**, 353–368.

Taylor, A. H., Watson, A. J., Ainsworth, M., Robertson, J. E. and Turner, D. R. 1991. A modelling investigation of the role of phytoplankton in the balance of carbon at the surface of the North Atlantic. *Global Biogeochem. Cycles* **5**, 151–171.

Wanninkhof, R. 1992. Relationship between wind speed and gas exchange over the ocean. *J. Geophys. Res.* **C97**, 7373–7382.

Weiss, R. F., Broecker, W. S., Craig, H. and Spencer, D. 1983. *Geosecs Indian Ocean expedition, hydrological data*, vol. 5, 48 pp., US Government Printing Office, Washington, DC.